PHILOSOPHICAL TRANSACTIONS OF THE ROYAL SOCIETY B

Phil. Trans. R. Soc. B (2005) **360**, 2095–2108
doi:10.1098/rstb.2005.1741
Published online 24 October 2005

From GCM grid cell to agricultural plot: scale issues affecting modelling of climate impact

Christian Baron[1,*], Benjamin Sultan[2], Maud Balme[3], Benoit Sarr[4], Seydou Traore[4], Thierry Lebel[3], Serge Janicot[2] and Michael Dingkuhn[1]

[1]*CIRAD—Amis/Agronomie/Ecotrop, TA 40/01, Avenue Agropolis 34398 Montpellier cedex 05, France*
[2]*IRD—Laboratoire d'Océanographie et du Climat: Expérimentation et Approche Numérique (LOCEAN)—UMR 7159 (CNRS/IRD/UPMC/MNHN) Université Pierre et Marie Curie, Case 100, 4 Place Jussieu 75252 Paris cedex 05, France*
[3]*IRD—Laboratoire d'étude des Transferts en Hydrologie et Environnement (LTHE)—UMR (CNRS/IRD/INPG/UJF), BP 53, 38 041 Grenoble cedex 09, France*
[4]*Centre AGRHYMET, BP 11011 Niamey, Republic of Niger*

General circulation models (GCM) are increasingly capable of making relevant predictions of seasonal and long-term climate variability, thus improving prospects of predicting impact on crop yields. This is particularly important for semi-arid West Africa where climate variability and drought threaten food security. Translating GCM outputs into attainable crop yields is difficult because GCM grid boxes are of larger scale than the processes governing yield, involving partitioning of rain among runoff, evaporation, transpiration, drainage and storage at plot scale. This study analyses the bias introduced to crop simulation when climatic data is aggregated spatially or in time, resulting in loss of relevant variation. A detailed case study was conducted using historical weather data for Senegal, applied to the crop model SARRA-H (version for millet). The study was then extended to a 10°N–17° N climatic gradient and a 31 year climate sequence to evaluate yield sensitivity to the variability of solar radiation and rainfall. Finally, a down-scaling model called LGO (Lebel–Guillot–Onibon), generating local rain patterns from grid cell means, was used to restore the variability lost by aggregation. Results indicate that forcing the crop model with spatially aggregated rainfall causes yield overestimations of 10–50% in dry latitudes, but nearly none in humid zones, due to a biased fraction of rainfall available for crop transpiration. Aggregation of solar radiation data caused significant bias in wetter zones where radiation was limiting yield. Where climatic gradients are steep, these two situations can occur within the same GCM grid cell. Disaggregation of grid cell means into a pattern of virtual synoptic stations having high-resolution rainfall distribution removed much of the bias caused by aggregation and gave realistic simulations of yield. It is concluded that coupling of GCM outputs with plot level crop models can cause large systematic errors due to scale incompatibility. These errors can be avoided by transforming GCM outputs, especially rainfall, to simulate the variability found at plot level.

Keywords: millet; drought; West Africa; grain yield; biomass; aggregation

1. INTRODUCTION

Climate has a strong influence on agricultural production, considered as the most weather-dependent of all human activities (Oram 1989; Hansen 2002), with socio-economical impacts whose severity varies from one region to another (Ogallo *et al.* 2000). These impacts are particularly strong in developing countries in the tropics that in many cases are exposed to high variability in climate like the monsoon system over West Africa and India and the El Niño–southern oscillation (ENSO) influence over the American continent (Challinor *et al.* 2003), and where poverty increases the risk and the impact of natural disasters (UNDP 2004). This is, especially, true in the Sahel where rainfed crop production is the main source of food and income and where means to control the crop environment are largely unavailable to farmers: irrigation is rarely an option and use of mechanization, fertilizers and other off-farm inputs are low (Ingram *et al.* 2002). In addition, the Sahel is currently affected by a food deficit crisis resulting from a rapidly growing population combined with stagnant yields of pearl millet, the main source of food and income of the Sahelian people, over the last few decades (De Rouw 2004) leading to a decrease of food production per capita (World Bank 1997).

The food crisis in the Sahel has been aggravated by the long-term drought of the last few decades (Nicholson 1986), and global climate change further increases the uncertainty of the region's development (Bazzaz & Sombroek 1996). Substantial progress has been made in understanding the variability of rainfall in West Africa, characterized mainly by both a strong

* Author for correspondence (christian.baron@cirad.fr).

One contribution of 17 to a discussion meeting issue 'Food crops in a changing climate'.

© 2005 The Royal Society

inter-annual variability and by periods of long-lasting droughts, such as the years 1970–1997 (Lebel *et al.* 2003), by factoring in surface characteristics (Zheng & Eltahir 1998) and in particular the interactions between ocean and atmosphere (Folland *et al.* 1986; Janicot *et al.* 2001). Knowledge about the interactions between the atmosphere and its underlying sea and land surfaces (Neelin *et al.* 1998), skills in modelling the global climate (Palmer *et al.* in press), and progress in the measurement of tropical near-surface waters (McPhaden *et al.* 1998) now provide a degree of predictability of climate fluctuations at a seasonal lead time in many parts of the world (Hansen 2002) by using comprehensive, coupled models of the atmosphere, oceans and land surface (Palmer *et al.* in press) or regional statistical schemes (Ward 1998; Fontaine *et al.* 1999; Ogallo *et al.* 2000). There is also increasingly more proof of climate change based on observed increases in global surface temperatures during the twentieth century, and significant inter-annual climate variability observed in many regions of the globe (Salinger 1994; Salinger *et al.* 1997), especially in tropical latitudes, caused by events such as the 1982/1983 and 1997/1998 El Niño and the 1991 Mount Pinatubo volcanic eruption (WMO 1995, 1998).

Considering the potential benefits of climate predictions to agriculture (Sivakumar *et al.* 2000; Hansen 2002) and the impacts of anthropogenic climate change on the Sahel, in particular the changing intensity, frequency and duration of rainy events (Trenberth *et al.* 2003), it appears crucial to orient the research efforts to the linkage between the two fields of research: meteorology and agriculture. This linkage was one of the objectives and achievements of the PROMISE (predictability and variability of monsoons and agricultural and hydrological impacts) project, funded by the European Union IV Framework Environment Programme, with partners from research in meteorology, hydrology and agriculture (http://ugamp.nerc.ac.uk/promise/). However, although there is worldwide agreement on the need for climate prediction for agriculture (Sivakumar *et al.* 2000), and although there has been significant progress in modelling agricultural and climatic processes and some of there interactions, the full integration of these two kinds of models still poses major problems due to the very different spatial and temporal scales at which processes happen. Seasonal climate predictions are made by using coupled or forced general circulation models (GCMs) to produce monthly or daily weather on scales with a spatial resolution of 200 km (Challinor *et al.* 2003), whereas most crop models simulate the impact of environmental factors on process rates at the plot level (Monteith 2000). The issues related to the linkage between GCMs and crop models fall into two categories: (i) related to deriving appropriate input information from GCMs for crop models (e.g. scale adaptation of data; validation with ground-based observations that may be unavailable, of poor quality or heterogeneous; Challinor *et al.* 2003), and (ii) the effect of scale *per se* on the laws that govern processes relevant to crop behaviour, such as the partitioning of rainfall into runoff, evaporation, drainage, stock replenishment and finally crop transpiration which is the key to crop productivity; Condon *et al.* 2004).

The objective of this study is to characterize potential yield simulation errors arising from disparate scales when coupling crop models with GCM outputs, and to explore approaches to resolve these problems. By using SARRA-H (Dingkuhn *et al.* 2003; Sultan *et al.* 2005), a crop model simulating radiation-driven and water-limited yield, we conduct sensitivity experiments on the response of simulated, attainable yield of millet in the Sahel to different aggregation levels of climate inputs.

2. MATERIAL AND METHODS

The deterministic crop model SARRA-H was applied to spatially distributed, historical, daily weather records (1950–1980) for dry areas in West Africa (10°N–18°N, or about 1000–300 mm annual rainfall), including the Guinea savannah, Sudan savannah and Sahel zones. Model sensitivity experiments were conducted to analyse the response of attainable (water, temperature and radiation limited) yield of millet, the most important cereal in the region, to different aggregation levels of climate inputs.

(a) *The crop model SARRA-H*

SARRA-H (Dingkuhn *et al.* 2003; Sultan *et al.* 2005) is a crop modelling platform recently developed from SARRA, the water balance model frequently used by agronomists and agro-meteorologists in West Africa for zoning and risk analyses (Affholder 1997; Baron *et al.* 1999) and yield forecasting (Samba 1998). The platform serves to assemble simple crop models from a library of modules and to apply them with the help of utilities such as sensitivity analysis and parameter optimization tools, database management and graphic interfaces. SARRA-H based models typically simulate attainable yields deterministically at the field scale (case of the millet model used here), but may also be stochastic and operate at variable temporal and spatial scales. Extrapolation from plot to region is routinely done by Agrhymet (Niamey) for agro-meteorological forecasting using the DHC system, which includes the SARRA water balance as central component (Samba 1998; Samba *et al.* 2001). The millet crop model was structured to enable such applications as well, but with greater physiological detail. Only details relevant to this particular version are described.

(i) *Soil water dynamics*

The model simulates at daily increments water runoff using an empirical threshold of 20 mm (Baron *et al.* 1996). The water not running off and not evaporating from the soil surface is partitioned among storage, deep drainage and transpiration. The soil is divided into a 20 cm top layer used to simulate evaporation and a layer of variable thickness representing the wetted zone. Water holding capacity of the soil between wilting point (pF = 4.2) and field capacity (pF = 3.0) is calibrated from available soil data, and was set to 100 mm m^{-1} for this study to represent a sandy soil. The root front, which descends at empirical rates depending on the growth stage, follows the wetting front but is also limited by it. Water extraction from the soil consists of two additive components, surface evaporation and extraction from the root zone through transpiration. Fraction ground cover is used to partition evaporative demand acting on the soil and the plant. Ground cover is computed from simulated leaf area

index (LAI) and an extinction coefficient K_{df} according to Beer–Lamberts's law (Vose *et al.* 1995).

(ii) *Plant water use and drought simulation*

Drought level is evaluated from fraction of transpirable soil water (FTSW) (Sinclair & Ludlow 1986) calculated for the bulk root zone, which is the relative degree of soil humidity between wilting point (FTSW = 0) and field capacity (FTSW = 1). This variable feeds back as a reducing factor on plant transpiration using FAO guidelines (P-factor system; Allen *et al.* 1998) and on carbon assimilation. Maximum evapotranspiration of the soil and canopy, achieved when the canopy is closed due to high LAI, is set with a crop factor K_c with potential evapotranspiration (PET) according to FAO guidelines for different crop species (Doorenbos & Pruitt 1977; Doorenbos & Kassam 1979). Intermediate transpiration levels during canopy establishment are a function of ground cover calculated from LAI.

(iii) *Carbon assimilation and partitioning*

Potential assimilation rates are calculated from ground cover, solar radiation and radiation use efficiency (Sinclair & Muchow 1999) before applying the drought related reduction. After subtraction of a temperature and biomass-dependent maintenance respiration term (Penning de Vries *et al.* 1989), biomass is partitioned during vegetative stage between root, stem and leaves according to empirical, allometric rules (Samba *et al.* 2001). Grain filling, however, is simulated with somewhat more detail to allow for variable harvest index, by determining sink capacity during pre-floral stages and inducing leaf senescence after flowering when sink capacity exceeds current assimilation rate. Leaf biomass is converted to leaf area using specific leaf area (Penning de Vries *et al.* 1989; Asch *et al.* 1999) whose dynamics are simulated on the basis of a genetic minimum and maximum value.

(iv) *Phenology*

Although, the model is capable of simulating variable crop cycle duration by taking into account photoperiod sensitivity, a fixed thermal time corresponding to about 90 days was used in this study to simulate millet, thus corresponding to an improved cultivar (Morel 1992; Dingkuhn *et al.* in press). Thermal time was calculated by assuming a base temperature of 10 °C (Clerget *et al.* 2004).

(v) *Model calibration and validation*

The crop model has been calibrated and validated on several independent experimental datasets for field grown millet in Senegal (Sultan *et al.* 2005). Biomass and grain production, as well as soil water extraction are simulated satisfactorily under different water regimes in researcher-managed trials. Indeed, for the same site at Bambey (Senegal) simulations of grain yield for three consecutive years and several water irrigation regimes, including rainfed situations explain almost 90% of the variance of observed grain yield ($R^2 = 0.89$; see Sultan *et al.* 2005). Simulation of water extraction of the crop from the soil also corresponded well to observations. These attainable yields, exceeding 4 tonnes of grain per hectare under optimal resources, however, are much higher than average farmers' yields that are affected by many unknown, biotic and abiotic factors. Consequently, the model simulates fairly accurately the (upper) envelope function of farmers' yields versus water resources, but not the scatter of points under the envelope (Sultan *et al.* 2005).

(b) *Onset date and length of the crop cycle*

In previous studies (Sultan & Janicot 2003; Sultan *et al.* 2005), it was demonstrated that the date of monsoon onset in the Sahel, about 22 June, varies little among years and sites (11 d standard deviation), as opposed to the large variability of the onset of the first rains, which can be several weeks to months earlier (see discussions in §4 of Sultan *et al.* 2005). The choice of sowing date is linked to varietal type (early, variable dates for traditional, photoperiod sensitive materials; fixed, hydrologically safe dates for materials having constant duration; Dingkuhn *et al.* in press). Because we chose a 'modern', 90 days varietal type for the simulations, a sowing date coinciding with the onset of monsoon rains (22 June) was most appropriate and was applied to the entire study. This mean date and its inter-annual variability are very similar to the onset date of the rainy season in northern Nigeria as defined by the criterion of minimal risk of false starts, requiring renewed sowing (Ati *et al.* 2002).

This choice of crop is obviously only one among many possible agronomic scenarios that need to be considered for studies on climate impact. More information is also needed on the spatial variability of onset dates for the rainy season. Our choice is sufficient, however, for the present purpose of evaluating bias and loss of information on variability associated with aggregation of weather variables.

(c) *Climate data*

Crop simulations were based: (i) on daily rainfall amount at stations located on the West African domain and (ii) on synoptic stations measuring several meteorological parameters at 2 m from ground such as global radiation (R_g), insolation (Ins), surface wind speed (W_s), humidity (maximum and minimum: H_{max} and H_{min}) and temperature (mean, maximum and minimum: T_{mean}, T_{max} and T_{min}) used to compute PET. The extended set of variables is also needed to simulate the crop's carbon budget that determines biomass build-up. These daily data have been compiled by the regional centre Agrhymet for 1950–1980 for 278 rain gauges and 86 synoptic stations. The data was used to run 31 year sequences of crop simulations, either for individual stations using daily inputs (control runs) or for spatially (grid cell) or temporally (10 d) aggregated data. Spatial aggregation was done for ensembles of stations falling into a common grid cell (principle of nearest gridpoint) of the size frequently used by global circulation models (GCM), e.g. 2.8°×2.8° which is a typical grid size from GCM such as ARPEGE--CLIMAT (Deque *et al.* 1994). Aggregation analyses were also conducted for 1°×1° grid cells but since results were very similar to those based on GCM grid cells, they are not presented here. Although there is a dilemma as to whether gridpoint output of a GCM represents a point or a spatial average (Katz 2002), we assume in this study that GCM outputs look like area-averaged precipitation as GCM output is intended to represent a grid box. This question of the interpretation of GCM gridpoint output, crucial for precipitation with high variability on small space and time scales, has been discussed by Katz (2002) reviewing evidence that GCM output is somewhere between a point and the entire grid box.

(d) *Computations and statistical analysis*

Aggregation of weather variables (for either rainfall alone or for all variables used in PET calculation) was done for populations of values, either based on spatial entities (GCM grid cells) or temporal entities (10 day periods). All the different runs of the study is described in table 1. A comparison of mathematical means and weighted means

Table 1. Description of the different runs of the study.

	meteorological variables (excluding rainfall)	rainfall
control run	daily observations from synoptic stations	daily observations from synoptic stations
EXP1	area-averaged daily observations	area-averaged daily observations
EXP2	1950–1980 averaged daily observations	daily observations from synoptic stations
EXP3	daily observations from synoptic stations	1950–1980 averaged daily observations
EXP4	10 days averaged observations	daily observations from synoptic stations
EXP5	daily observations from synoptic stations	10 days averaged observations

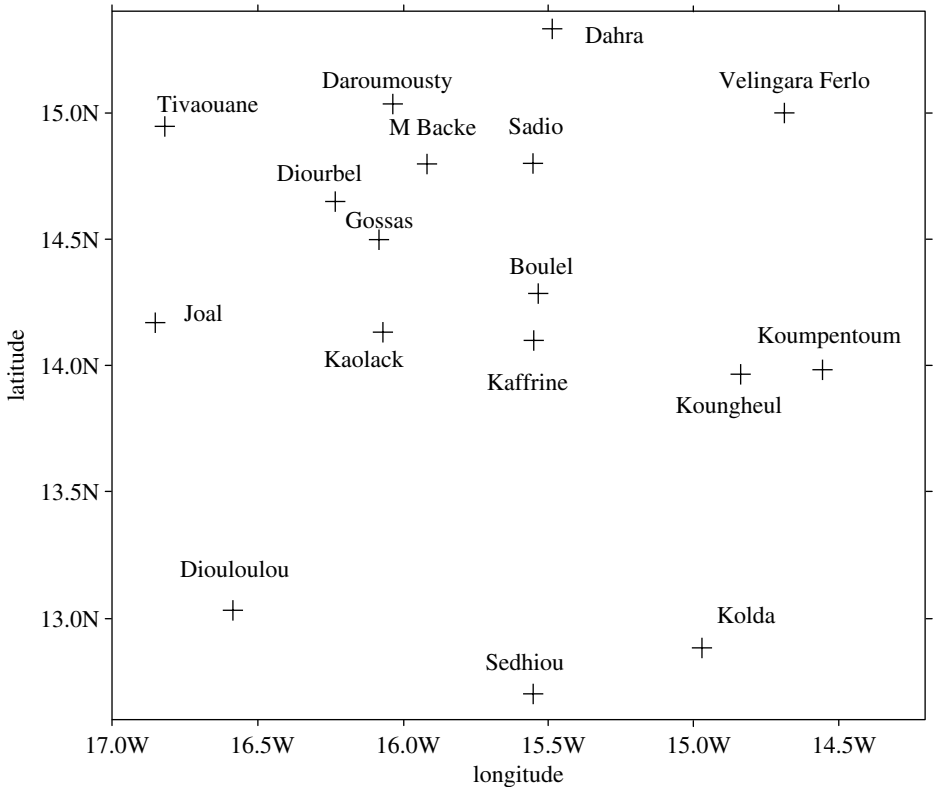

Figure 1. Spatial distribution of rain gauges in Senegal used to simulate yield variability in a virtual GCM box.

by krigging of stations falling into a common grid cell (not presented) gave no significant differences (case study in Senegal, $N=17$; cell shown in figure 1), and we therefore used simple averages in aggregation exercises.

When comparing yields simulated with non-aggregated (control run; see table 1) and aggregated (EXP1; see table 1) agro-meteorological input data, yield differences were evaluated using the relative standard error $\varepsilon_s = \sigma_\varepsilon^2/\sigma_c^2$, where σ_ε^2 is the error variance defined as

$$\sigma_\varepsilon^2 = \frac{1}{N-1}\sum_{i=1}^{N}(e_i - c_i)^2,$$

where c_i represents the control run value for the year i and $\bar{c}$ the 31 years average ($N=31$), and e_i the experimental run value for the year i and σ_c^2 is the control run variance defined as:

$$\sigma_c^2 = \frac{1}{N-1}\sum_{i=1}^{N}(c_i - \bar{c})^2.$$

The ε_s values are between 0 (the experimental run is similar to the control run) and $+\infty$. The 1 value indicates that the experimental run reproduces none of the inter-annual variability of the control run (each value of the experimental run is equal to the mean result of the 31 control runs). To quantify the loss of information on yield variability, we computed the inverse of the coefficient of determination: $1-R^2$ (ICD; in percentage). The ICD values are located between 0 (the variability of the experimental run is similar that of the control run) and 100% (none of the inter-annual variability of the control run is reproduced). Statistical analyses were, generally, conducted with *R* software (www.r-project.org).

3. RESULTS AND DISCUSSION

(a) *Effect of spatial and temporal aggregations of weather data on simulated crop yield*

In this section, we quantify systematic errors obtained when using aggregated climate inputs to force the crop model SARRA-H to simulate annual yield of millet in Sahel.

(i) *Yield predictions using spatially aggregated rainfall data*

In order to quantify the bias in yield simulation brought about by spatially aggregating rainfall, a case study was conducted in Senegal where 17 rain gauges were available inside a square (crosses in figure 1) whose size is similar to a GCM grid box from 17°W to 14.2°W and from 12.6°N to 15.4°N. A smaller box of about 1°

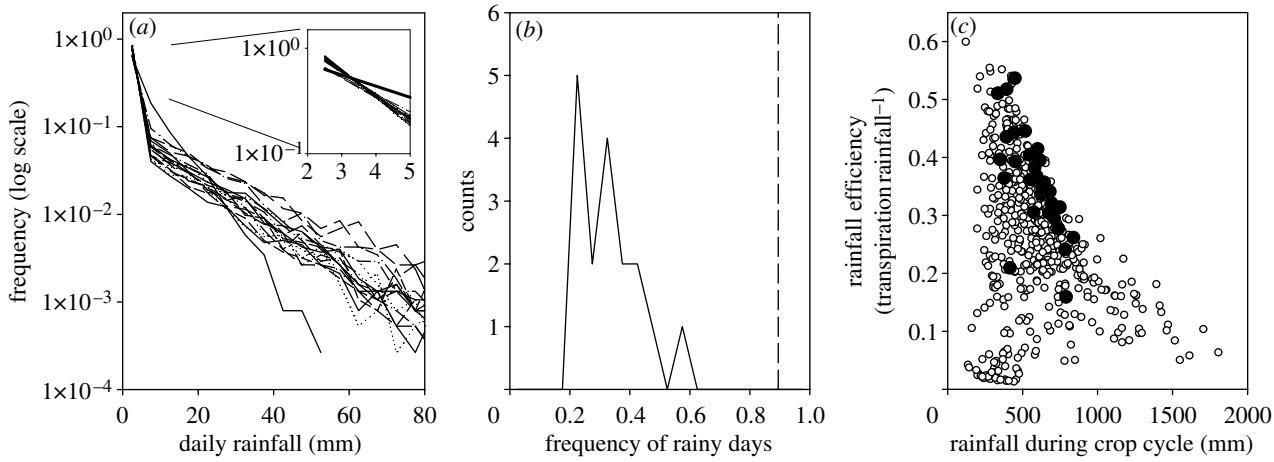

Figure 2. (*a*) Daily rainfall distribution from June to September (JJAS) during 1950–1980 for the individual 17 stations of the GCM box of figure 1 (dotted lines) and for of the 17-station average (solid line). (*b*) Histogram of rain event frequency for the same 31 years. On the horizontal axis, 0 indicates that it never rains and 1 that it rains every day. The vertical line represents the value for the 17-station average. (*c*) Relationship between rainfall efficiency (transpiration rainfall^{-1}) and total rainfall amount during crop cycle, simulated for 17 stations (dots) the 17-station average (circles).

square including 13 stations (not shown) was also defined to represent an intermediate level of aggregation.

Figure 2*a* compares the daily rainfall distribution within the rainy season (June to September) for 1950–1980 (dotted lines) with the distribution of the mean observations for 17 stations (bold line). Since there is rarely more than one rainfall event contributing to the daily totals at a given site and date, the non-averaged distributions are roughly indicative of the size of individual rainfall events, which in turn strongly affect the partitioning of precipitation among runoff, evaporation, drainage and crop transpiration as simulated by the crop model SARRA-H. Averaged values for 17 sites distorted distributions by: (i) underestimating the frequency of rainless days (top left corner of graph, (ii) overestimating the occurrence of intermediate rainfall events between 5 and 20 mm (that would benefit the crop most) and strongly underestimating the occurrence of events larger than 30 mm (that would lead to high runoff).

Figure 2*b* shows the histogram of the probability of rainy days within the wet season for the 17 stations. Zero on the horizontal axis indicates the absence of rains, 0.5 indicates one rainy day in two, and 1.0 indicates rains on every day. Most of the stations are situated between 0.2 and 0.4, or rains every 5–2.5 days. The corresponding value for all sites averaged (vertical line in figure 2*b*) is 0.9, indicating that within the observed area it rains almost every day.

Seasonal rainfall characteristics are thus strongly affected by spatial aggregation. This distortion can not only be expected for aggregated ground observations, but also for GCM-based simulations that do not take into account local rain storms. According to the crop model, the distortion of rainfall intensity and frequency distribution brought about by aggregation results in an overestimation of agronomically effective precipitation, defined as the fraction of water transpired by the crop (figure 2*c*).

In order to evaluate the error caused by rainfall aggregation when simulating crop yield, the SARRA-H model was run with non-aggregated (control run; see table 1) and averaged rain data (EXP1; see table 1) for the 17 sites (figure 3). For each point representing one year out of 31, averaging was thus performed either for the input variable (daily rainfall) or the output variable (biomass or grain yield). Both grain yield and crop biomass were strongly overestimated when averaged rainfall was used, particularly where yields were low (figure 3*a*). Overestimations were in the order of 30–40% between 400 and 700 mm rainfall totals, but lower for less than 400 and greater than 700 mm. Thus, the yield bias caused by aggregation was highly variable.

The overestimation was slightly larger for the 2.8° square as compared to the 1° square (not presented). The simulation error can been estimated by computing the relative bias (r_b) defined by

$$r_b = 1\bar{c}\left[\frac{1}{N}\sum_{i=1}^{N}(e_i - c_i)\right],$$

where c_i represents the control run value for the year i and $\bar{c}$ the 31 years average ($N=31$), and e_i the experimental run value for the year i.

Rainfall aggregation on a 2° grid box introduced a mean overestimation of 26% ($r_b=0.26$) for biomass at crop maturity and 28% for grain yield. Overestimations were only slightly smaller (24% for biomass and 26% for grain yield) when aggregation was performed on a 1° grid box (sub-sample from the same area, data not presented).

According to simulations with the crop model, this bias has three causes.

(i) High daily precipitation (greater than 30 mm) results in high runoff which is ineffective for plant growth and unavailable for deep infiltration of the soil, resulting in a shallow wetting front and consequently, a shallow root system.
(ii) Intermediate rainfall (10–30 mm d^{-1}) contributes strongly to soil wetting because it causes little runoff but exceeds evapotranspiration (ET) significantly.

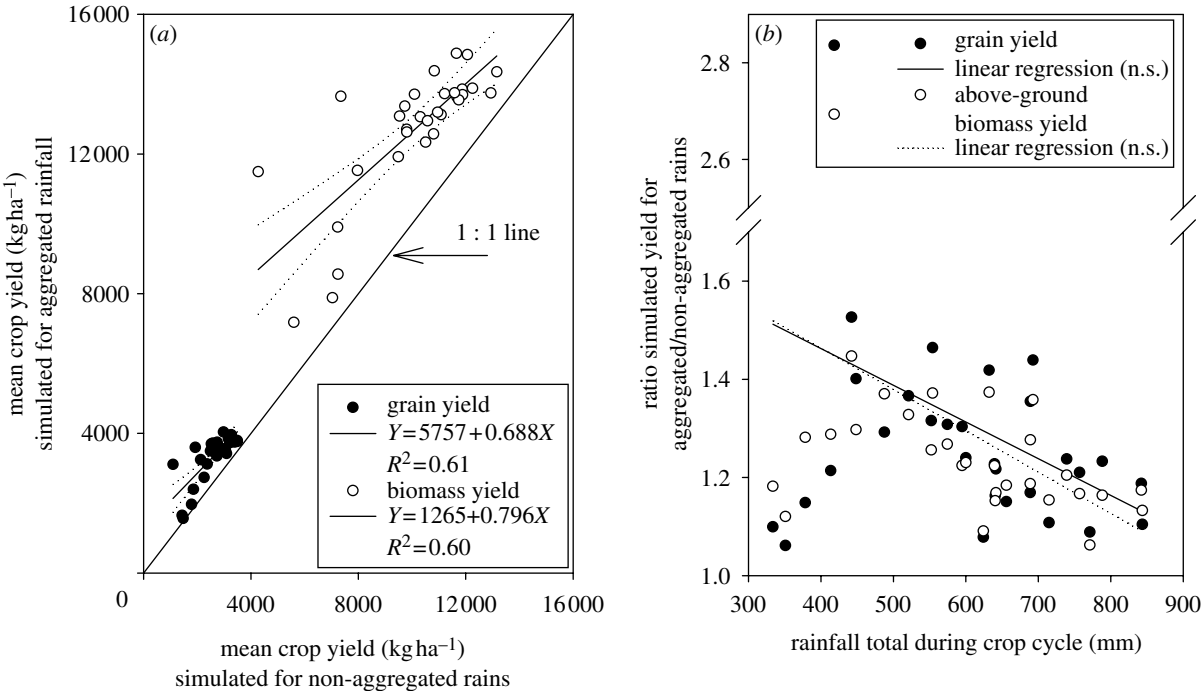

Figure 3. (*a*) Relationship between annual crop grain yield (filled symbols) and biomass (open) simulated with aggregated rainfall inputs (vertical axis) and individual inputs for stations (horizontal). Linear regression lines are flanked by 95% confidence intervals using Sigma Plot v.9 software. (*b*) Relationship between the yield bias caused by rainfall aggregation (vertical, derived from data on left graph) and total rainfall during the crop cycle.

(iii) Low rainfall (1–10 mm d^{-1}) is highly effective for plant growth but contributes little to deep soil wetting because it is similar to the daily ET.

Since rainfall aggregation increased the apparent fraction of low to intermediate rainfall, it led to an overestimation of rainfall efficiency (defined here as the ratio of transpiration to rainfall). Interestingly, this bias strongly affected the absolute yield values but only slightly the relative, inter-annual variability of simulated yields, as indicated by a coefficient of variation (CV) among 31 years of 29% for spatially aggregated and 35% for non-aggregated rainfall. Consequently, the average bias caused by aggregation was similar for dry and wet years. It, therefore, seems that although for a given site and year attainable crop yield is extremely sensitive to intra-seasonal rainfall distribution, its inter-annual variability is mainly controlled by annual rainfall totals. Similarly, spatial yield variability among the 17 sites on the grid unit was correlated with rainfall totals. This can be explained with the strong, decreasing trend in annual rainfall totals observed for all sites during the 31 years considered in this study (Lebel *et al.* 2003).

The analysis of the impact of aggregated climate inputs was extended to the entire semi-arid (Sudan savannah and Sahel) zone of West Africa for 1950–1980 (figure 4), using 284 weather stations or, on average, 10.5 weather stations per 2.8° grid unit. As in figure 2, grain yield simulations were performed either with averaged climate data for each grid unit (figure 4*a*), or with individual stations followed by averaging simulated yields (figure 4*b*). The results show a pronounced north–south gradient in attainable yields due to the regional distribution of annual rains, indicating that rainfall is increasingly yield-limiting as the crop is planted further north. The overestimation brought about by spatial averaging of rainfall is greatest in the dry areas (14°N–17°N; sometimes exceeding 40%) but negligible in lower latitudes of the studied zone. Large overestimations were also observed for the coastal zones (Senegal and Mauritania).

(ii) *Sensitivity of simulated yield to climatic variability on a north–south gradient and in time*

Crop biomass and yield are not only dependent on rainfall and soil water storage. If we consider only the effects of climate variables and not those of on-farm parameters (e.g. mineral inputs and crop protection), attainable yield is mainly limited by water, energy or both. In the SARRA-H crop model, intercepted light energy acts as the engine of growth whereas water deficit acts as a break on growth. Depending on which effect is stronger, yield can be pre-dominantly radiation-driven or water-limited. On the north–south climatic gradient of semi-arid west Africa, the relative weight of the energy and water terms is likely to change with latitude. In the following, we evaluate this latitudinal effect on yield and the probability of encountering different situations within a GCM grid box.

Three reference sites on the north–south gradient were chosen (Bougouni, 11.42°N; Bamako, 12.53°N; Niamey, 13.48°N). The distance between the southern and the northern sites is about the length of a GCM grid box (2.06°). In 1950–1980, mean, annual rainfall totals were highest in Bougouni (1133 mm), intermediate in Bamako (915 mm) lowest in Niamey (541 mm). For the three stations, two simulation experiments were performed: (i) the crop model runs with daily, 31 year, means of meteorological inputs (R_g, Ins, W_s, T_{mean}, T_{max}, T_{min}, H_{max}, H_{min}) while rainfall is

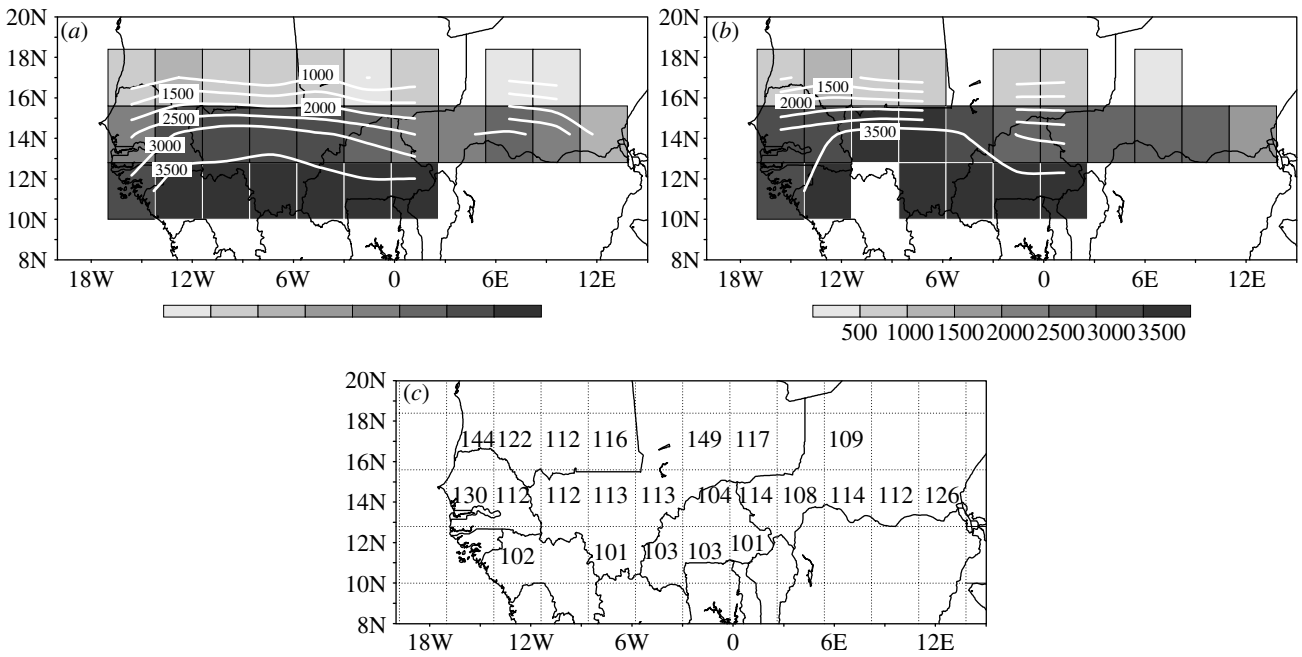

Figure 4. 1950–1980 mean yield (kg ha^{-1}) simulated by (*a*) aggregating daily rainfall inputs or (*b*) aggregating yield outputs for virtual GCM boxes. (*c*) The ratio between the mean yield of (*b*) and (*a*) is presented as a percentage.

Table 2. Relative standard error (ε_s) and the inverse of the coefficient of determination (ICD) between the control run and the experimental run with 31 years mean daily meteorological inputs (left term) and 31 years mean rainfall inputs (right term) for three stations: Niamey, Bamako and Bougouni.

	Niamey		Bamako		Bougouni	
	mean met	mean rain	mean met	mean rain	mean met	mean rain
ε_s(%)	30.1	84.4	79.1	79.1	99.3	10.0
ICD (%)	12.2	33.7	64.1	74.8	94.7	3.3

not averaged across years (EXP2; see table 1); and (ii) the model runs with daily, 31 year, means of rainfall while meteorological variables are not averaged across years (EXP3; see table 1). The yield differences to the control run (no variables are averaged) were evaluated using the relative standard error ε_s, and the ICD was used to quantify the loss of information on yield variability brought about by aggregation of model input data (table 2), as described in §2*d*.

Figure 5 plots the two experimental runs against the control run. Results differed markedly among the three stations. When all meteorological variables except rainfall were averaged (i) (figure 5*a*), the inter-annual yield variability was well reproduced in Niamey, the driest site, but it almost disappeared in Bougouni with quasi-constant attainable yield at a high level near the biological potential of the crop. The value of ε_s increased from north to south (Bougouni) where about 90% of the inter-annual yield variability escaped prediction (table 2). At the intermediate site Bamako this loss of variability was still 60%. The reverse case (ii), with meteorological variables averaged and rainfall not, produced opposite results with a ε_s decreasing from north to south. Although, the variability of yield in Niamey (dry site) remained in part preserved with a loss of only about 30% (refer to ICD in table 2), ε_s was high because low yield values were systematically overestimated. At the wet site of Bougouni the loss of inter-annual variability was less than 10%.

These two experiments point out a differential sensitivity of simulated crop yield depending on latitude and thus, on annual rainfall. In the semi-arid zone of Niamey, biomass and yield are mainly controlled by the seasonal characteristics of the rainfall as previously reported by Sultan *et al.* (2005), whereas attainable yield is insensitive to variability of other agro-meteorological variables. In the southern zone of Bougouni, rainfall becomes non-limiting and attainable yield depends on solar radiation. At the intermediate location Bamako, yield simulation is sensitive to both solar radiation and water. This diversity of situations within the same GCM grid box constitutes a risk of considerable bias when aggregated climate inputs are used to predict yield.

The study of the relative effect of water and solar radiation on attainable yield was extended to the whole West African domain. Figure 6 shows the modulation of simulated yield (from the control run) by rainfall and solar radiation for more than 30 synoptic stations distributed over the Sahel and savannah zones of West Africa for 1950–1980.

Plotting attainable grain yield against rainfall totals for the duration of the crop cycle (figure 6*a*), a bi-phasic envelope pattern was obtained consisting of an

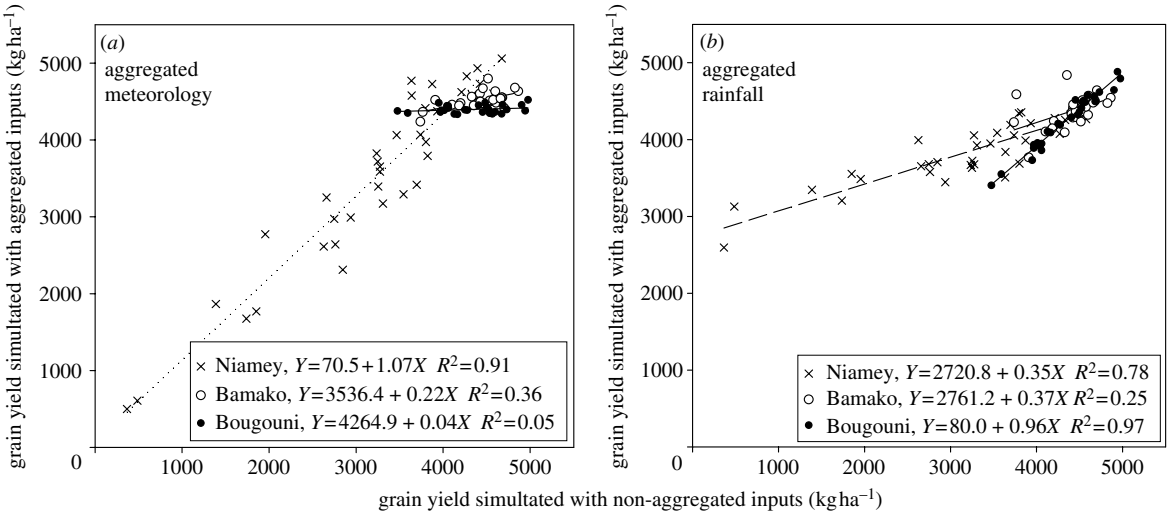

Figure 5. Relationship between grain yield (kg ha^{-1}) simulated for 1950–1980 for aggregated weather inputs (vertical axis, experimental run) and station specific inputs (horizontal axis, control run). (*a*) Aggregation of meteorological inputs (except rainfall) for GCM-type grid boxes for 31 years. (*b*) Aggregation of rainfall inputs. Data points and linear regressions for Niamey (circles), Bamako (triangles) and Bougouni (crosses).

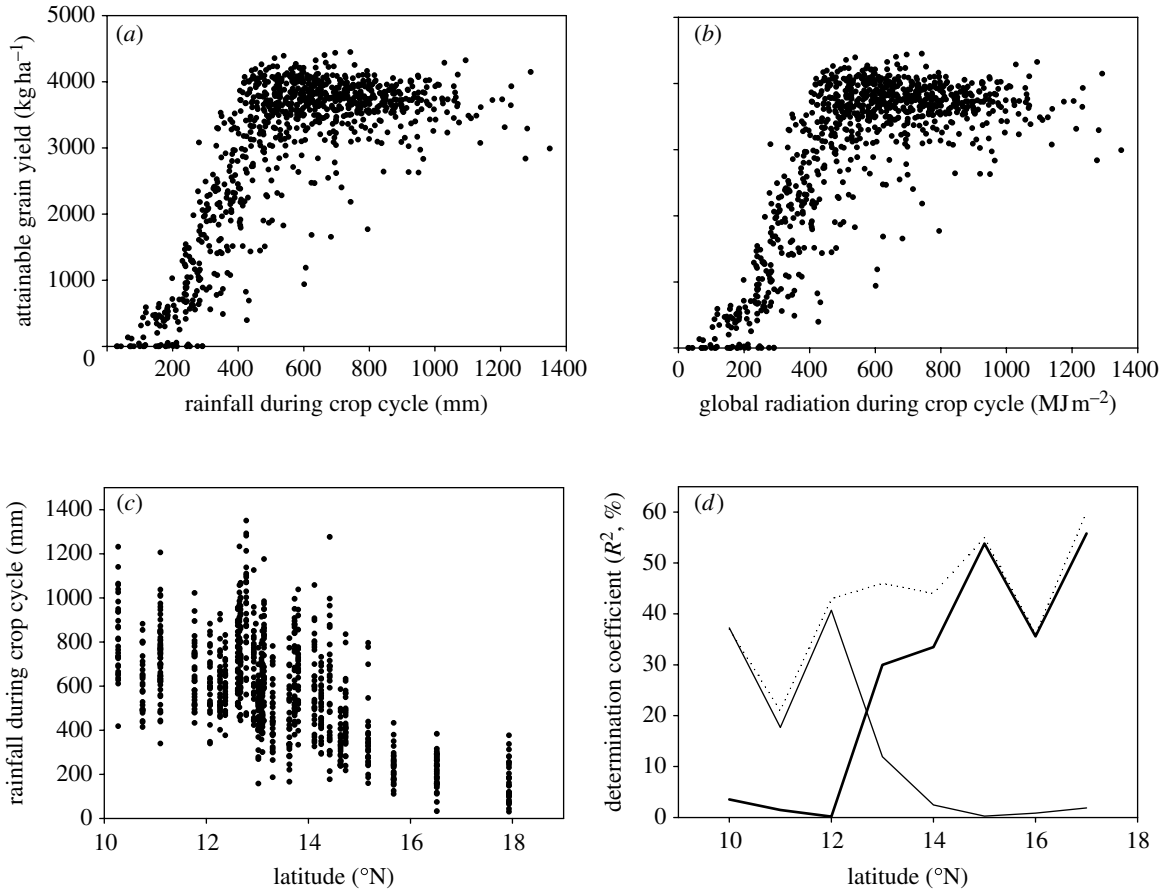

Figure 6. (*a*) Relationship between simulated grain yield and rainfall per crop cycle for 30 stations in West Africa for 1950–1980. (*b*) As in (*a*) but using global radiation as independent variable. (*c*) Relationship between rainfall per crop cycle and latitude (°N). (*d*) Coefficient of determination (R^2 expressed as percentage) for the linear regression of grain yield versus rainfall (bold line), versus global radiation (thin line) and versus both rainfall and global radiation (dotted line). Linear regressions were computed for ensembles of stations grouped at 1° latitude intervals.

exponential relationship between 0 and 500 mm and a slightly decreasing plateau for higher rainfall totals. Beneath this envelope curve (consisting of cases with good rainfall distribution) there was considerable scatter (cases of unfavourable distribution; Sultan *et al.* 2005). The slope of the plateau was due to decreasing solar radiation as rainfall was frequent, a situation typical of lower latitudes. Plotting attainable grain yield against cumulative solar radiation (figure 6*b*), the envelope curve showed a linear, increasing trend in the

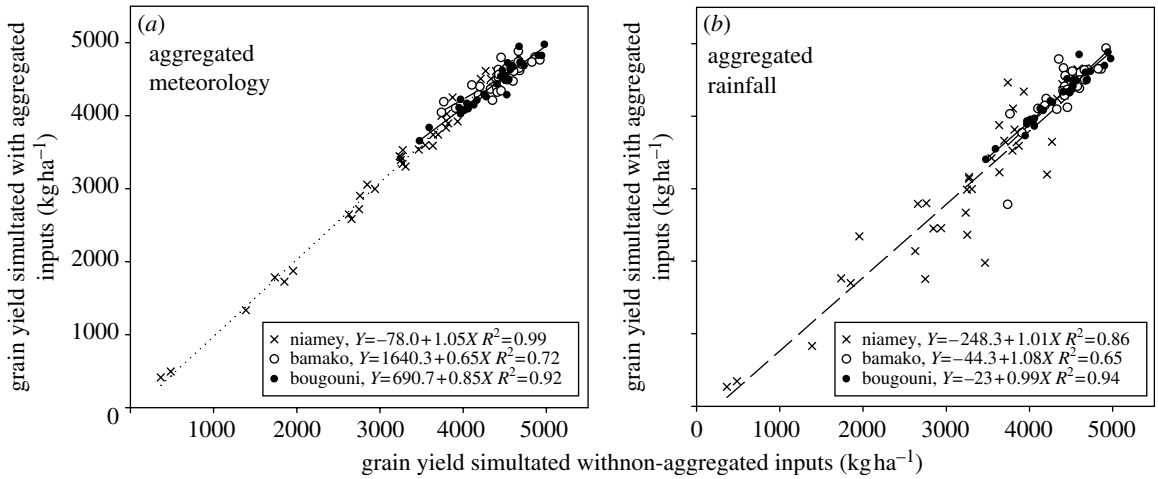

Figure 7. Relationship between grain yield (kg ha^{-1}) simulated for aggregated weather inputs (vertical) and station specific inputs (horizontal) for Niamey (crosses), Bamako (open circles) and Bougouni (filled circles) as in figure 4, using temporal (10 days) aggregation of weather inputs in experimental runs instead of spatial aggregation.

observed range of 1500–2300 MJ m^{-2}, with much scatter underneath that was mainly due to insufficient rain, typical of higher latitudes (figure 5*c*). For most stations between 10°N and 13°N and most years, rainfall exceeded 500 mm per crop cycle, whereas for most stations north of 15°N and most years, rainfall was less than 500 mm. Figure 6*c* also shows a strong inter-annual variability of rainfall between 13°N and 15°N with rainfall totals between 100 and 1300 mm per cycle. Across the spectrum of latitudes, the relative importance of the water and energy terms in the determination of attainable yield was evaluated through the computation of the coefficient of determination (R^2) for the yield versus rainfall and yield versus solar radiation linear regression analyses, applied to latitude classes of 1° (figure 6*d*). This analysis shows that seasonal rainfall totals do not explain attainable-yield variations between 10°N and 12°N while they become the predominant factor beyond 13°N and explain more than 50% of yield variations at 15°N and 17°N. Solar radiation totals explained about 40% of yield variation at 10°N and 12°N but virtually none beyond 14°N. At 13°N and 14°N, the variability of attainable yield depends on both solar radiation ($R^2=12\%$) and rainfall totals ($R^2=30\%$), the R^2 of the multiple, linear regression for both factors is about 46%. Nonlinear regression analyses would have probably provided greater R^2 values for rainfall effects but our objective here is to demonstrate the potential diversity of situations within a GCM grid cell, and not necessarily fully quantitative factor contributions that may be modulated by many additional, biotic and abiotic factors at farm level.

By using the same three stations on a latitudinal transect, we also investigated the sensitivity of yield simulation to temporal aggregation of climate inputs. Two simulation experiments were performed by: (i) running the crop model with observed, daily rainfall and 10 day means of other meteorological variables (EXP4; see table 1); and (ii) running with 10 day means of rainfall and daily meteorological variables (EXP5; see table 1). Statistical analyses were performed as described above.

Using 10 day means of meteorological variables (except rainfall) introduced only marginal errors and virtually no bias (figure 7*a*). The largest error was observed for the intermediate station in Bamako (table 3). Large losses of yield variability were observed, however, when daily rainfall was averaged on a 10 day basis, particularly for Bamako and Niamey (figure 7*b*). This was associated with a strong bias of yield prediction as indicated by the slope of the relationship deviating substantially from 1.

This simulation experiment showed that differential, site specific sensitivity of simulated yield to climate variables is associated with differential sensitivity to temporal aggregation of climate inputs. Thus, a millet crop grown in a place like Bougouni, will be less sensitive to temporal aggregation than one grown in Bamako or Niamey, where rainfall is the limiting factor. For these two latter sites, sensitivity to 10 day aggregation of rainfall can be explained by strong day-to-day variability of rainfall which is smoothed by the temporal average. The large variability of rainfall among synoptic stations in the Sahel was documented by Le Barbé & Lebel (1997) and Lebel *et al.* (2003) and attributed to properties of the rain events. These authors show that the erratic temporal behaviour of rainfall is linked to their convective origin, mainly controlled by a succession of convective systems. While these systems last for more than 24 h and account for more than 60% of the total cloud cover over the Sahel (Mathon & Laurent 2001), they generally produce rain for only a few hours at a given location, due to their high speed of displacement, and rain periods are separated by several hours or days with no rainfall (Lebel *et al.* 2003). Another synoptic feature modulating rainfall over the Sahel are the Easterly Waves (Reed *et al.* 1977) responsible for two intra-seasonal modulations of both rainfall and atmospheric signals, propagating westward at 3–5 days and 6–9 days (Diedhiou *et al.* 1998, 1999). As for the spatial aggregation of climate variables (§3*a*(i)), intra-seasonal, temporal aggregation tends to smooth rainfall distribution, resulting in less and shorter dry periods

Table 3. Relative standard error (ε_s) and the inverse of the coefficient of determination (ICD) between the control run and the experimental run with decadal meteorological inputs (left term) and decadal rainfall inputs (right term) for three stations: Niamey, Bamako and Bougouni.

	Niamey		Bamako		Bougouni	
	mean met	mean rain	mean met	mean rain	mean met	mean rain
ε_s(%)	3.5	35.4	34.4	71.8	11.3	10.9
ICD (%)	1.5	19.3	28.3	35.0	8.3	5.5

and fewer extreme values to which crop yield is sensitive.

(b) *Downscaling of aggregate climate to accommodate crop models*

Future forecasting will face critical issues of scale because GCM outputs will come at different resolutions, and may thus be quite different from the weather experienced by the crop at the plot level. Integrated climate–crop modelling systems, therefore, need to handle appropriately the loss of variability caused by the difference between scales. This can potentially be achieved in two different ways: (i) by a scaling up of crop modelling, as proposed by Challinor *et al.* (in press) who designed a crop model able to run at a spatial scale comparable to the resolution of GCMs, or (ii) by scaling down of GCM outputs by various dynamic, empirical or statistic–dynamic methods. The first option (i) is technically simpler but relies on the possibility to partition rainfall into effective (transpiration) and ineffective fractions in the absence of the information needed to mechanistically predict partitioning, such as size of rainfall events. This is, generally, possible on the basis of empirical, region-specific relationships between rainfall and water available for crop growth, while assuming that event size distribution varies little. Such a model would require specific calibration for different climates and soils. Because of the strong variability of rainfall in space and time and its variable weight in determining grain yield in semi-arid West Africa (Lebel *et al.* 2003), our focus in this section will be on option (ii), namely, downscaling of aggregate climate data. We will use the example of Senegal to evaluate a statistical downscaling method based on rainfall event properties and dynamics.

(i) *Statistical and dynamic downscaling*

While GCMs reproduce the dominant patterns of the inter-annual variability of the coupled ocean–atmosphere system at low resolution, such as the ENSO phenomenon, they have much lesser skills at higher spatial resolution (Grotch & MacCracken 1991). Zorita & Storch (1999) pointed out several causes of the models' failure at the regional scale such as: (i) inadequate representation of topography and land–sea distribution, (ii) application of large scale parameterization of energy flow to smaller scales, and (iii) inadequate representation of sub-grid scale processes such as rainfall, infiltration or runoff. However, sub-grid processes are strongly linked to human activities that affect ecology and local climate (Zorita & von Storch 1999). This is especially true in the Sahel where rainfall is highly variable in space and time due to its convective nature (Guillot & Lebel 1999) and where measurements are scarce (Lebel & Amani 1999). Lebel *et al.* (2000) conducted a comparative analysis of the variability of observed and rainfall predicted by GCM in semi-arid Africa using the climate model LMD-6 (Polcher & Laval 1994) at a resolution of 1.6° in latitude and of 3.75° in longitude. They pointed out errors in predicting the seasonal cycle (wet season too early and too long) and meso-scale convective systems which are responsible for 95% of annual rainfall in semi-arid regions such as Niamey (Laurent *et al.* 1998). The latter problem affects strongly the day-to-day distribution of rainfall.

To accurately represent the impact on agricultural processes of GCM-derived climate scenarios, downscaling techniques are required that enhance large-scale information with effects and processes characteristic at small scales (Von Storch 1995). Downscaling techniques belong to three different groups:

(i) dynamic methods requiring the use of limited-area models simulating weather at meso-scale (20–50 km) while taking into account regional characteristics (such as the MAR model developed for West Africa by Gallée *et al.* 2004);
(ii) statistical downscaling using empirical relationships between the large-scale circulation and the local climate, using stochastic weather generators (Wilks & Wilby 1999), regression models (linear methods such as canonical analyses and nonlinear methods such as neural networks) and weather models (e.g. clustering and analogue methods); and
(iii) statistical–dynamic methods that combine dynamic and empirical methods (Zorita & von Storch 1999).

The choice of a class of model is often largely conditioned by the targeted scales. Here, the focus is on reproducing the convective scale variability from areal averages available at the typical resolution of a climate model that performs downscaling from a few hundred kilometres to a few kilometres. A model developed by Onibon *et al.* (2004) was used to that end.

(ii) *The Lebel–Guillot–Onibon downscaling model*

Using high-resolution data collected in the semi-arid region of Niamey (Niger), Guillot & Lebel (1999) proposed a space–time model, allowing the disaggregation of large-scale estimates derived from satellite images or GCM outputs. The initial version used turning band algorithms and was not intended to perform simulations conditioned on known areal

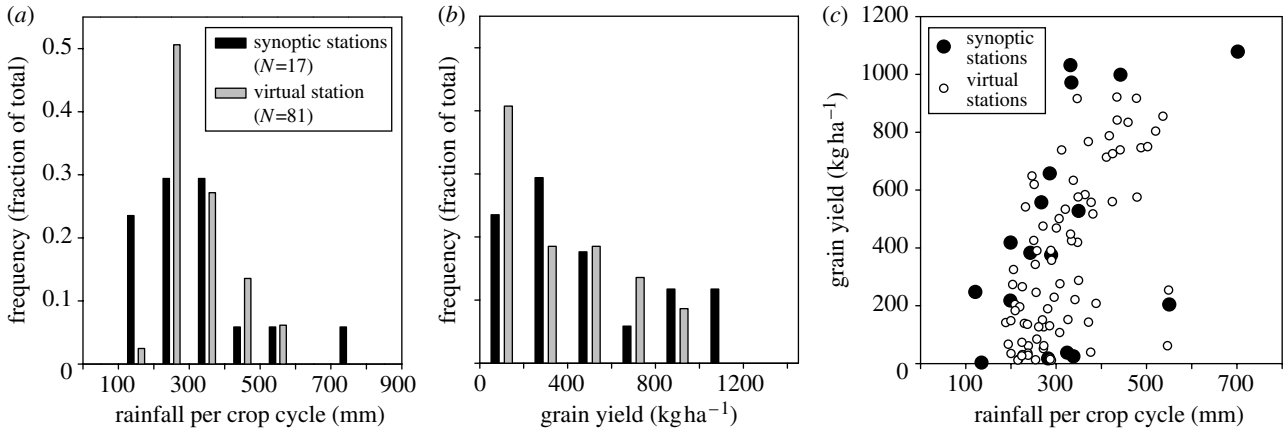

Figure 8. (*a*) Distribution of total rainfall during crop cycle for 17 synoptic stations and 81 virtual stations reconstituted from GCM grid cell mean. (*b*) Distribution of grain yield simulated for the same data. (*c*) Relationship between grain yield and total rainfall per crop cycle, simulated for 1972 for a 2.8°×2.8° GCM grid cell (refer to figure 1) with rainfall observed for 17 stations (closed circles) and reconstituted, virtual stations (open circles).

characteristics. Onibon *et al.* (2004) presented a new version that performs conditional simulations of precipitation fields in the context of Gaussian transformed functions. This method allows constructing diverse scenarios of precipitation fields when only a spatially averaged estimate is known over a given area, using the coupling of a Gibb's sampler with an acceptation–rejection algorithm. The model, which generates series of spatial patterns for a given area average, was successfully validated with field observations in the Niamey area (Onibon *et al.* 2004).

(iii) *Applying the Lebel–Guillot–Onibon model to the Senegal case study*

The direct transposition of the Lebel–Guillot–Onibon (LGO) model in Senegal raises a question about the accuracy of its parameters outside the central Sahel boundaries, although rainfall totals are very similar. The model builds on knowledge on Sahelian meso-scale convective systems, based on 13 years of EPSAT-Niger ground measurements (Lebel *et al.* 1992). No such high-resolution measurements are available in the Senegal and we, therefore, used daily rainfall data instead of rain event data, and assumed that the same covariance parameters and rainfall characteristics apply (see Guillot & Lebel 1999 for values). The case study boxes in Senegal include no coastal areas to avoid ocean influence, but the ratio of meso-scale convective systems and local oceanic systems is unknown. The present study is, therefore, of preliminary nature, aiming to provide proof of concept but not a final solution to downscaling.

(iv) *Realistic yields*

The simulations presented here use 1972 as example. For each day of the year where rainfall was recorded anywhere in the grid boxes shown in figure 1, disaggregated precipitation fields are established on a grid of virtual weather stations, either for the larger GCM grid box or for the 1°×1° grid box using the Lebel–Guillot–Onibon (LGO) model. Results seem encouraging (figure 8). The spatial variability, observed at the pixel scale, is well restored by the disaggregated precipitation fields and the LGO model offers a large spectrum of spatial patterns for a single area average, allowing different crop scenarios. As regards yield simulations, they are realistic compared to those simulated with the measured rainfall data.

The LGO model seems to be a useful way to overcome the scale gap between GCM outputs and agronomic crop models operating at the plot level. In order to develop a fully operational, coupled modelling system, however, the LGO model must be validated and if necessary recalibrated for the areas targeted, and its coupled execution with the crop model automated. On this basis, low resolution GCM outputs can be directly translated into agronomic impact parameters without bias resulting from scale gaps.

(c) *Implications for impact predictions of climate change*

The results indicate that the bias in crop yield prediction attributable to insufficient resolution of agro-meteorological data is much greater for rainfall than for the other meteorological variables, and consequently, much greater in water-limited than radiation-limited environments. Consequently, if this bias is not taken into account, the negative agricultural impact of drought would be underestimated at an economically important scale (10–50%), considering that mean yield increases in the order of 5% achieved with improved varieties or cultural practices are considered as major. This bias can be avoided by down-scaling techniques such as the disaggregation methodology presented here (which is tedious because it greatly increases the number of simulations and requires climate specific calibration of the down-scaling model), or empirical coefficients for bias compensation (which reduces the genericity of the model). Empirical techniques may in some cases be more practical and sufficiently robust (Challinor *et al.* 2003, 2004) because, as our results indicate, the systematic error coming from aggregation can be large in absolute terms, but is much smaller in terms of inter-annual variability. However, attention must be given to the fact that 2.8°×2.8° grid cells are large enough to mask significant climatic gradients.

With respect to the objective of predicting agricultural impact, climate modellers should not be satisfied with accurately predicting general trends of annual or seasonal rainfall totals and radiation means (already a remarkable achievement), but should also consider their intra-seasonal distribution. If it is unrealistic to expect GCM simulations to descend to the scale of local rainstorms, supplemental models are needed to derive local patterns from larger scale dynamics in a generic approach. The issue is, of course, not to predict a particular rain event, but to accurately represent system behaviour at the relevant spatial and temporal scales on a probabilistic basis. A typology of intra-seasonal patterns of rainfall distribution in the Niamey area has been developed and applied to the SARRA-H crop model in a precursor study (Sultan *et al.* 2005).

The present study on scale effects on crop yield simulation is preliminary in the sense that it considered only a specific crop and varietal type (photoperiod insensitive, short duration millet). Different results can be expected when using a crop with greater phenological plasticity, providing greater flexibility in sowing date and lower (but more stable) yields (Dingkuhn *et al.* in press). We also focused primarily on effects of rainfall and solar radiation because these variables are responsible for attainable-yield limitations on north–south gradients in West Africa. Temperature is another agrometeorological factor that has strong impacts on yield in the tropics, particularly through effects on crop duration (thus limiting biomass build-up) and maintenance respiration (limiting the yield ceiling) (Penning de Vries *et al.* 1989). These effects, accounted for by SARRA-H, are small for a crop like millet mainly grown in water-limited environments but strongly affect crops grown in warm, low-radiation environments such as rice. High air temperatures can shorten crop duration considerably below the agronomic optimum but the development of varieties having appropriate duration under such conditions is a relatively easy task for breeders. By contrast, detrimental effects on rice yields of rising nocturnal temperatures, as observed recently in southeast Asia and chiefly attributed to crop respiration (Peng *et al.* 2004), are more difficult to correct and need to be taken into account in future impact studies. For temperature effects, spatial resolution of data may be less of a problem than temporal resolution, because temperature related processes in crops are very sensitive to diurnal T amplitudes (Dingkuhn *et al.* 1995).

Lastly, this study did not take into account carbon dioxide levels in the atmosphere because the focus was on historical climate date, and because millet, having a C_4-type metabolism, is comparatively insensitive to this parameter (Wolfe 1994). It is also unlikely that carbon dioxide concentrations will show variability sensitive to aggregation.

4. CONCLUSION

This study evaluated the bias and loss of variability in crop yield simulation at the plot scale, brought about by aggregating weather variables used as model inputs in space or time. This is a problem to be considered when forcing crops models with GCM outputs on large grid cells. Blending small precipitation fields into much larger grid cells alters the size distribution of rain events and thus changes the proportion of runoff, drainage, crop transpiration, soil evaporation and storage. In particular, the over-representation of small and mid size events through aggregation increases the crop transpiration term in the water balance, resulting in an overestimation of yield. Rainfall was much more sensitive to aggregation than were other meteorological variables like solar radiation, temperature and air humidity, and consequently, yield overestimations were greatest in the most water-limited environments. The bias can be corrected by reintroducing micro-variability of precipitation by disaggregating GCM pixels into populations of virtual stations.

Currently available tools and approaches to generate plot-scale size distribution and frequency of rainfall events for large grid cells are insufficiently available and operational for routine impact predictions. Their development would be more important for water limited than for humid environments where the main yield limiting factor is solar radiation, a variable that is less sensitive to aggregation than rainfall.

This study was supported by the European Community research projects PROMISE and AMMA.

REFERENCES

Affholder, F. 1997 Empirically modelling the interaction between intensification and climatic risk in semiarid regions. *Field Crop Res.* **52**, 79–93. (doi:10.1016/S0378-4290(96)03453-3.)

Allen, R. G., Pereira, L. S., Raes, D. & Smith, M. 1998 Crop evapotranspiration—guidelines for computing crop water requirements. *FAO Irrigation and drainage*, paper 56. Rome, Italy: FAO.

Asch, F., Sow, A. & Dingkuhn, M. 1999 Reserve mobilization, dry matter partitioning and specific leaf area in seedlings of African rice cultivars differing in early vigor. *Field Crop Res.* **62**, 191–202. (doi:10.1016/S0378-4290(99)00020-9.)

Ati, O. F., Stigter, C. J. & Oladipo, E. O. 2002 A comparison of methods to determine the onset of the growing season in northern Nigeria. *Int. J. Climatol.* **22**, 731–742. (doi:10.1002/joc.712.)

Baron C., Clopes A., Perez P., Muller B., Maraux F. 1996 Manuels d'utilisation de: SARRAMET 45 p, SARRABIL 35 p et SARRAZON 29 p, Montpellier, France: CIRAD.

Baron, C., Reyniers, F. N., Clopes, A. & Forest, F. 1999 Applications du logiciel SARRA à l'étude de risques climatiques. *Agric. Dév.* **24**, 89–97.

Bazzaz, F. & Sombroek, W. 1996 *Global climate change and agricultural production. Direct and indirect effects of changing hydrological, pedological and plant physiological processes*. Rome: Wiley, FAO.

Clerget, B., Dingkuhn, M., Chantereau, J., Hemberger, J., Louarn, G. & Vaksmann, M. 2004 Does panicle initiation in tropical sorghum depend on day-to-day change in photoperiod? *Field Crop Res.* **88**, 11–27. (doi:10.1016/j.fcr.2003.08.010.)

Challinor, A. J., Slingo, J. M., Wheeler, T. R., Craufurd, P. Q. & Grimes, D. I. F. 2003 Toward a combined seasonal weather and crop productivity forecasting system: determination of the working spatial scale. *J. Appl. Meteorol.* **42**, 175–192. (doi:10.1175/1520-0450(2003)042<0175:TACSWA>2.0.CO;2.)

Challinor, A. J., Wheeler, T. R., Craufurd, P. Q., Slingo, J. M. & Grimes, D. I. F. 2004 Design and optimisation of a large-area process-based model for annual crops. *Agr. Forest Meteorol.* **124**, 99–120.

Condon, A. G., Richards, R. A., Rebetzke, G. J. & Farquhar, G. D. 2004 Breeding for high water-use efficiency. *J. Exp. Bot.* **55**, 2447–2460. (doi:10.1093/jxb/erh277.)

De Rouw, A. 2004 Improving yields and reducing risks in pearl millet farming in the African Sahel. *Agric. Syst.* **81**, 73–93. (doi:10.1016/j.agsy.2003.09.002.)

Deque, M., Dreveton, C., Braun, A. & Cariolle, D. 1994 The ARPEGE/IFS atmosphere model: a contribution to the French community climate modelling. *Climate Dyn.* **10**, 249–266. (doi:10.1007/s003820050047.)

Diedhiou, A., Janicot, S., Viltard, A. & de Felice, P. 1998 Evidence of two regimes of easterly waves over West Africa and the Tropical Atlantic. *Geophys. Res. Lett.* **25**, 2805–2808. (doi:10.1029/98GL02152.)

Diedhiou, A., Janicot, S., Viltard, A., de Felice, P. & Laurent, H. 1999 Easterly wave regimes and associated convection over West Africa and the tropical Atlantic: results from NCEP/NCAR and ECMWF reanalyses. *Climate Dyn.* **15**, 795–822. (doi:10.1007/s003820050316.)

Dingkuhn, M., Sow, A., Samb, A., Diack, S. & Asch, F. 1995 Climatic determinants of irrigated rice performance in the Sahel. I. Photothermal and microclimatic responses of flowering. *Agr. Syst.* **48**, 385–410. (doi:10.1016/0308-521X(94)00027-I.)

Dingkuhn, M., Baron, C., Bonnal, V., Maraux, F., Sarr, B., Sultan, B., Clopes, A. & Forest, F. 2003 Decision support tools for rainfed crops in the Sahel at the plot and regional scales. In *Decision support tools for smallholder agriculture in sub-Saharan Africa—a practical guide* (ed. T. E. Struif Bontkes & M. C. S. Wopereis), pp. 127–139. The Netherlands: CTA Wageningen.

Dingkuhn, M., Singh, B. B., Clerget, B., Chantereau, J., Sultan, B. In press. Past, present and future criteria to breed crops for water-limited environments in West Africa. *Agr. Water Manage.* Published online 15 August 2005. See http://www.cropscience.org.au/icsc2004/symposia/1/1/448_dingkuhn.htm.

Doorenbos, J. & Pruitt, W. O. 1977 Guidelines to predicting water requirements. *FAO Irrigation and Drainage*, paper no. 24. Rome, Italy: FAO.

Doorenbos, J. & Kassam, A. H. 1979 Yield response to water. *FAO Irrigation and Drainage*, paper no. 33. Rome, Italy: FAO.

Folland, C. K., Palmer, T. N. & Parker, D. E. 1985 Sahel rainfall and worldwide sea temperature 1901–1985. *Nature* **320**, 602–607. (doi:10.1038/320602a0.)

Fontaine, B., Philippon, N. & Camberlin, P. 1999 An improvement of June–September rainfall forecasting in the Sahel based upon region April–May moist static energy content 1968–1997). *Geophys. Res. Lett.* **26**, 2041–2044. (doi:10.1029/1999GL900495.)

Gallée, H., Moufouma-Okia, W., Bechtold, P., Brasseur, O., Dupays, I., Marbaix, P., Messager, C., Ramel, R. & Lebel, T. 2004 A high resolution simulation of a West African rainy season using a regional climate model. *J. Geophys. Res.* **109**, D05108. (10.1029/2003JD004020.)

Grotch, S. & MacCracken, M. 1991 The use of general circulation models to predict regional climate change. *J. Clim.* **4**, 286–303. (doi:10.1175/1520-0442(1991)004<0286:TUOGCM>2.0.CO;2.)

Guillot, G. & Lebel, T. 1999 Disaggregation of Sahelian mesoscale convective system rain fields: further developments and validation. *J. Geophys. Res.* **104**, 31 533–31 551. (doi:10.1029/1999JD900986.)

Hansen, J. W. 2002 Realizing the potential benefits of climate prediction to agriculture: issues, approaches, challenges. *Agric. Syst.* **74**, 309–330. (doi:10.1016/S0308-521X(02)00043-4.)

Ingram, K. T., Roncoli, M. C. & Kirshen, P. H. 2002 Opportunities and constraints for farmers of West Africa to use seasonal precipitation forecasts with Burkina Faso as a case study. *Agric. Syst.* **74**, 331–349. (doi:10.1016/S0308-521X(02)00044-6.)

Janicot, S., Trzaska, S. & Poccard, I. 2001 Summer Sahel-ENSO teleconnection and decadal time scale SST variations. *Climate Dyn.* **18**, 303–320. (doi:10.1007/s003820100172.)

Katz, R. W. 2002 Techniques for estimating uncertainty in climate change scenarios and impact studies. *Climate Res.* **20**, 167–185.

Laurent, H., Jobard, I. & Toma, A. 1998 Validation of the satellite and ground based estimates of precipitation over the Sahel. *Atmos. Res.* **47–448**, 651–670. (doi:10.1016/S0169-8095(98)00051-9.)

Le Barbé, L. & Lebel, T. 1997 Rainfall climatology of the HAPEX-Sahel region during the years 1950–1990. *J. Hydrol.* **188–1189**, 43–73. (doi:10.1016/S0022-1694(96)03154-X.)

Lebel, T. & Amani, A. 1999 Rainfall estimation in the Sahel: what is the ground truth? *J. Appl. Meteorol.* **38**, 555–568. (doi:10.1175/1520-0450(1999)038<0555:REITSW>2.0.CO;2.)

Lebel, T., Sauvageot, H., Hoepffner, M., Desbois, M., Guillot, B. & Hubert, P. 1992 Rainfall estimation in the Sahel: the EPSAT Niger experiment. *J. Hydrol. Sci.* **37**, 201–215.

Lebel, T., Delclaux, F., Le Barbé, L. & Polcher, J. 2000 From GCM scales to hydrological scales: rainfall variability in West Africa. *Stoch. Environ. Res. Risk Assess.* **14**, 275–295. (doi:10.1007/s004770000050.)

Lebel, T., Diedhiou, A. & Laurent, H. 2003 Seasonal cycle and interannual variability of the Sahelian rainfall at hydrological scales. *J. Geophys. Res.* **108**, 8389. (doi: 10.1029/2001JD001580.)

Mathon, V. & Laurent, H. 2001 Life cycle of Sahelian mesoscale convective cloud systems. *Q. J. R. Meteor. Soc.* **127**, 377–406. (doi:10.1256/smsqj.57207.)

McPhaden, M. J. *et al.* 1998 The tropical ocean–global atmosphere observing system: a decade of progress. *J. Geophys. Res.* **103**, 14 169–14 240. (doi:10.1029/97JC02906.)

Monteith, J. L. 2000 Agricultural meteorology: evolution and application. *Agric. Forest Meteorol.* **103**, 5–9. (doi:10.1016/S0168-1923(00)00114-3.)

Morel, R. 1992 *Atlas agroclimatique des pays de la zone du CILSS, t.1, Notice et commentaires*. Niamey, Niger: Programme Agrhymet.

Neelin, J. D., Battisti, D. S., Hirst, A. C., Jin, F.-F., Wakata, Y., Yamagata, T. & Zebiak, S. 1998 ENSO theory. *J. Geophys. Res.* **103**, 14 261–14 290. (doi:10.1029/97JC03424.)

Nicholson, S. E. 1986 Climate, drought and famine in Africa. In *Food in Sub-Saharan Africa* (ed. A. Hansen & D. E. McMillan), pp. 107–128. Boulder: Lynne Rienner.

Ogallo, L. A., Boulahya, M. S. & Keane, T. 2000 Applications of seasonal to interannual climate prediction in agricultural planning and operations. *Agric. Forest Meteorol.* **103**, 159–166. (doi:10.1016/S0168-1923(00)00109-X.)

Onibon, H., Lebel, T., Afouda, A. & Guillot, G. 2004 Gibbs sampling for conditional spatial disaggregation of rain fields. *Water Resour. Res.* **40**, W08401. (doi:10.1029/2003WR002009.)

Oram, P. A. 1989 Sensitivity of agricultural production to climatic change, an update. *Climate Food Security*, pp. 25–44. Manila, The Philippines: IRRI.

Palmer, T. N. *et al.* 2004 Development of a European multi-model ensemble system for seasonal to inter-annual prediction (DEMETER). *Bull. Am. Meteorol. Soc.* **85**, 853–872.

Peng, S., Huang, J., Sheehy, J. E., Laza, R. C., Visperas, R. M., Zhong, X., Centeno, G. S., Khush, G. S. & Cassmann, K. G. 2004 Rice yields decline with higher night temperatures from global warming. *Proc. Natl Acad. Sci. USA* **101**, 9971–9975. (doi:10.1073/pnas.0403720101.)

Penning de Vries, F. W. T., Jansen, D. M., Ten Berge, H. F. M. & Bakema, A. 1989 *Simulation of ecophysiological processes of growth in several annual crops*, p. 291. Wageningen: PUDOC.

Polcher, J. & Laval, K. 1994 A statistical study of regional impact of deforestation on climate of the LMD–GCM. *Climate Dyn.* **10**, 205–219. (doi:10.1007/BF00208988.)

Reed, R. J., Norquist, D. C. & Recker, E. E. 1977 The structure and properties of African wave disturbances as observed during Phase III of GATE. *Mon. Weather Rev.* **105**, 317–333. (doi:10.1175/1520-0493(1977)105<0317:TSAPOA>2.0.CO;2.)

Salinger, M. J. 1994 Climate variability, agriculture and forests. *WMO technical note* **196**. Geneva: WMO.

Salinger, M. J., Desjardins, R., Jones, M. B., Sivakumar, M. V. K., Strommen, N. D., Veerasamy, S. & Lianhai, W. 1997 Climate variability, agriculture and forestry: an update. *WMO Technical Note* **199**, 51. Geneva: WMO.

Samba, A. 1998 Les logiciels Dhc de diagnostic hydrique des cultures. Prévision des rendements du mil en zones soudano-sahéliennes de l'Afrique de l'Ouest. *Sécheresse*, **9**, 281–288.

Samba, A., Sarr, B., Baron, C., Gozé, E., Maraux, F., Clerget, B. & Dingkuhn, M. 2001 La prévision agricole à l'échelle du Sahel. In *Modélisation des agro-écosystèmes et aide à la décision* (ed. E. Malézieux, G. Trébuil & M. Jaeger), pp. 243–262. Montpellier, France: Cirad and INRA.

Sinclair, T. R. & Ludlow, M. M. 1986 Influence of soil water supply on the plant water balance of four tropical grain legumes. *Aust. J. Plant Physiol.* **13**, 329–341.

Sinclair, T. R. & Muchow, R. C. 1999 Radiation use effciency. *Adv. Agron.* **65**, 215–265.

Sivakumar, M. V. K., Gommes, R. & Baier, W. 2000 Agrometeorology and sustainable agriculture. *Agr. Forest Meteorol.* **103**, 11–26. (doi:10.1016/S0168-1923(00)00115-5.)

Sultan, B. & Janicot, S. 2003 The West African monsoon dynamics. Part II: the pre-onset and the onset of the summer monsoon. *J. Clim.* **16**, 3407–3427. (doi:10.1175/1520-0442(2003)016<3407:TWAMDP>2.0.CO;2.)

Sultan, B., Baron, C., Dingkuhn, M. & Janicot, S. 2005 Agricultural impacts of large-scale variability of the west African monsoon. *Agr. Forest Meteorol.* **128**, 93–110. (doi:10.1016/j.agrformet.2004.08.005.)

Trenberth, K. E., Dai, A., Rasmussen, R. M. & Parsons, D. B. 2003 The changing character of precipitation. *Bull. Am. Meteorol. Soc.* **84**, 1205–1217. (doi:10.1175/BAMS-84-9-1205.)

UNDP 2004 Reducing disaster risk: a challenge for development. In *UNDP global report* (ed. M. Pelling). See http://www.undp.org/bcpr/disred/documents/publications/rdr/english/rdr_english.pdf.

Von Storch, H. 1995 Inconsistencies at the interface of climate impact studies and global climate research. *Meteorol. Z.* **4 NF**, 72–80.

Vose, J. M., Sullivan, N. H., Clinton, B. D. & Bolstad, P. V. 1995 Vertical leaf area distribution, light transmittance, and application of the Beer–Lambert law in four mature hardwood stands in the southern Appalachians. *Can. J. Forest Res.* **25**, 1036–1043.

Ward, M. N. 1998 Diagnosis and short-lead time prediction of summer rainfall in tropical north Africa at interannual and multidecadal timescales. *J. Clim.* **11**, 3167–3191. (doi:10.1175/1520-0442(1998)011<3167:DASLTP>2.0.CO;2.)

Wilks, D. S. & Wilby, R. L. 1999 The weather generation game: a review of stochastic weather models. *Prog. Phys. Geog.* **23**, 329–357. (doi:10.1191/030913399666525256.)

WMO 1995 The global climate system review: Climate system monitoring, June 1991–November 1993. Geneva: WMO.

WMO 1998 The global climate system review. December 1993–May 1996. Geneva: WMO. See http://www.wmo.ch/web/wcp/wcdmp/review/856rev.htm.

Wolfe, D. W. 1994 Physiological and growth responses to atmospheric carbon dioxide. In *Handbook of plant and crop physiology* (ed. M. Pessarakli), pp. 223–242. New York: Marcel Dekker, Inc.

World Bank, 1997 African development indicators. Washington DC, USA.

Zheng, X. & Eltahir, E. A. 1998 The role of vegetation in the dynamics of West African monsoons. *J. Clim.* **11**, 2078–2096.

Zorita, E. & von Storch, H. 1999 The analog method—a simple statistical downscaling technique: comparison with more complicated methods. *J. Clim.* **12**, 2474–2489. (doi:10.1175/1520-0442(1999)012<2474:TAMAAS>2.0.CO;2.)